Supplementary information

c-Met-targeted near-infrared fluorescent probe for real-time depiction and dissection of perineural invasion and lymph node metastasis lesions in pancreatic ductal adenocarcinoma xenograft models

Dan Li[1], Meilin Yang[1], Mingzhu Liang[1,2,3], Chaoming Mei[1], Yujing Lin[4], Yitai Xiao[1], Fan Yang[1], Yuechuan Chen[1], Fen Wang[5*], Junjie Mao[2*], Zhongzhen Su[1,6*]

1. Guangdong Provincial Key Laboratory of Biomedical Imaging and Guangdong Provincial Engineering Research Center of Molecular Imaging, The Fifth Affiliated Hospital of Sun Yat-sen University, Zhuhai, Guangdong Province 519000, China.

2. Center for Interventional Medicine, The Fifth Affiliated Hospital of Sun Yat-sen University, Zhuhai, Guangdong Province 519000, China

3. Department of Radiology, The Fifth Affiliated Hospital of Sun Yat-sen University, Zhuhai, Guangdong Province 519000, China.

4. Department of Pathology, The Fifth Affiliated Hospital of Sun Yat-sen University, Zhuhai, Guangdong Province 519000, China.

5. Department of Pathology, The First Affiliated Hospital of Sun Yat-sen University, Guangzhou, Guangdong Province 510080, China

6. Department of Ultrasound, The Fifth Affiliated Hospital of Sun Yat-sen University, Zhuhai, Guangdong Province 519000, China

Dan Li, Meilin Yang, and Mingzhu Liang contributed equally to this article.

*Corresponding authors: Zhongzhen Su, Junjie Mao, Fen Wang

Zhongzhen Su, Department of Ultrasound, The Fifth Affiliated Hospital of Sun Yat-sen University, Zhuhai, Guangdong Province 519000, China, Tel: 86-07562528232, E-mail: suzhzh3@mail.sysu.edu.cn. Junjie Mao, Center for Interventional Medicine, The Fifth Affiliated Hospital, Sun Yat-sen University, Zhuhai, Guangdong Province 519000, China, Tel: 86-07562526187, E-mail: maojunj@mail.sysu.edu.cn. Fen Wang, Department of Pathology, The First Affiliated Hospital of Sun Yat-sen University, Guangzhou 510080, China, Tel: 86-7562528106, E-mail: wangfen5@mail.sysu.edu.cn.

1. Supplementary methods

Database analysis of c-Met expression

The mRNA expression data corresponding to the c-Met gene were explored in the GEPIA2 database (http://gepia2.cancer-pku.cn/). *MET* expression was compared between human pancreatic cancer tissue and normal pancreatic tissue, and the correlation between *MET* and other genes (*CEACAM5, VEGFR2, HER2, EGFR), uPAM, PDL1*) that have been applied as probe targets was also analysed.

The Human Protein Atlas (https://www.proteinatlas.org/) was used to analyse c-Met expression in many human solid tumours. The expression of c-Met protein was compared with that of other proteins that have been used as imaging targets for PDAC (https://www.tcpaportal.org/).

2. Supplementary table

Table S1. c-Met expression and clinicopathological features of PDAC patients

Characteristics	Total (n = 106)	c-Met expression		Chi-square	*p*
		Low (n = 17)	High (n = 89)		
Sex				0.020	0.889
Male	67	11	56		
Female	39	6	33		
Age (years)				1.612	0.204
≤60	46	5	41		
>60	60	12	48		
Tumour size (cm)				0.227	0.634
≤4	76	13	63		
>4	30	4	26		
TNM stage				1.881	0.404
I	49	10	39		
IIa	17	3	14		
IIb/III/IV	40	4	36		
PNI lesions				0.751	0.386
Negative	46	9	37		
Positive	60	8	52		
LNM lesions				2.163	0.141
Negative	71	14	57		
Positive	35	3	32		

*$p < 0.05$ (Chi-square Test)

3. **Supplementary figures**

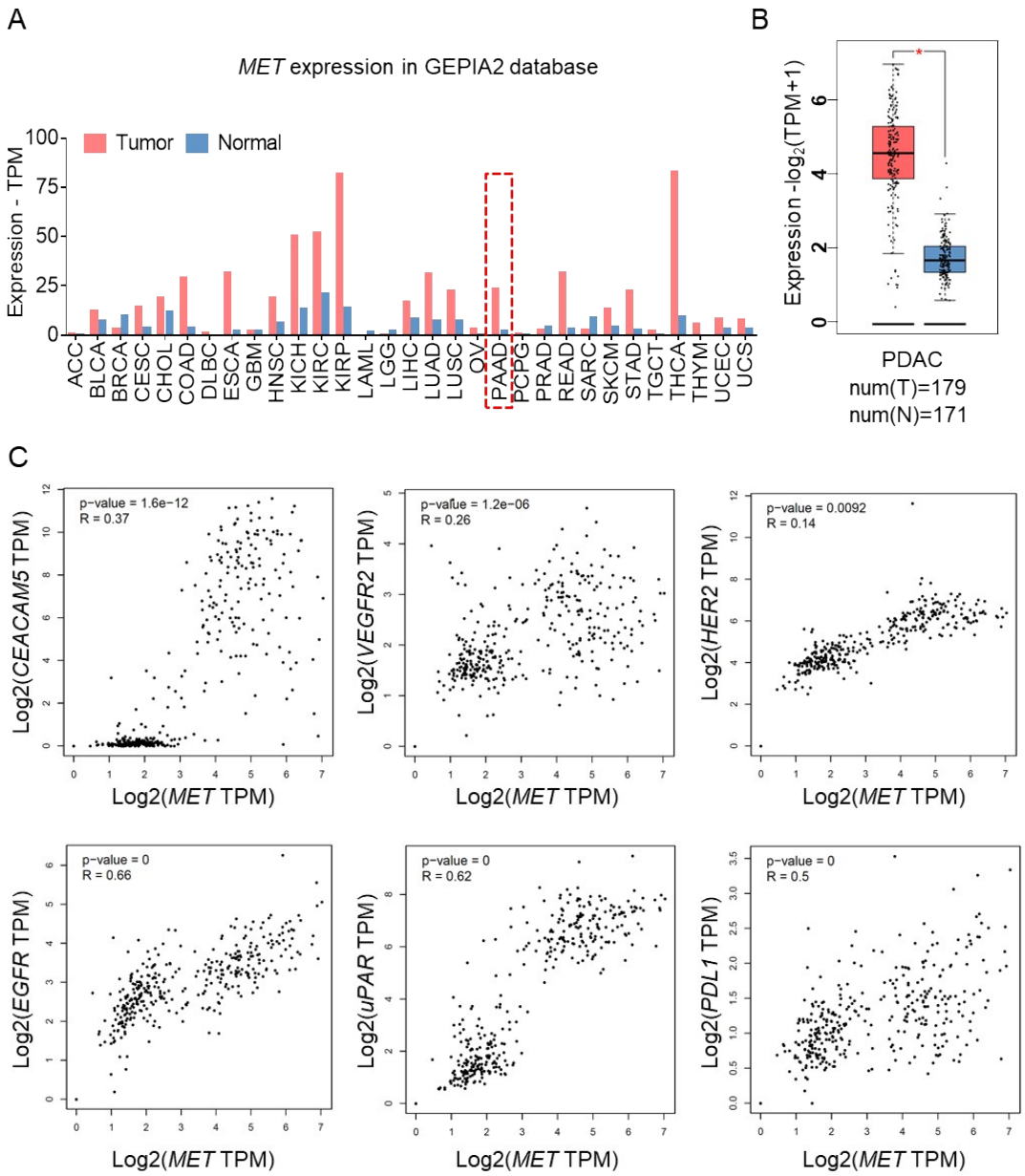

Figure S1. *MET* expression in GEPIA2 database. (A) The *MET* gene expression profile across all tumour samples (red plot) and paired normal tissues (blue plot) (TCGA). The height of the bar represents the median expression of a certain tumour type or normal tissue; PAAD (pancreatic adenocarcinoma) is 23.73, while normal is 2.31. (B) The *MET* expression in PDAC was higher than that in normal pancreas tissue. T: tumour; N: normal tissue. (C) Correlation analysis of *MET* and other genes, such as *CEACAM5*, *VEGFR2*, *HER2*, *EGFR*, *uPAR*, and *PDL1*.

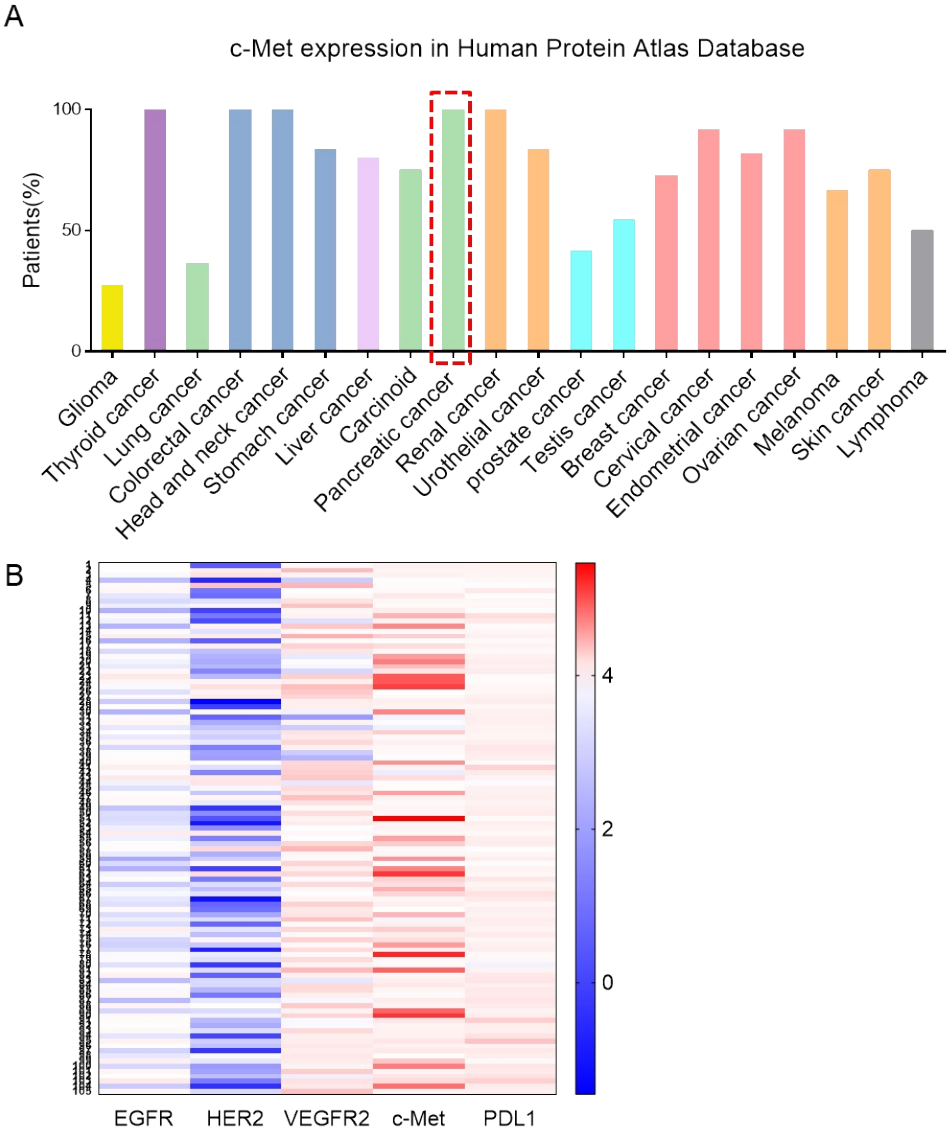

Figure S2. c-Met expression in proteomics database. (A) Human Protein Atlas Database analysis of c-Met in PDAC. (B) The expression of c-Met and other targets (EGFR, HER2, VEGFR2, PDL1) in PDAC.

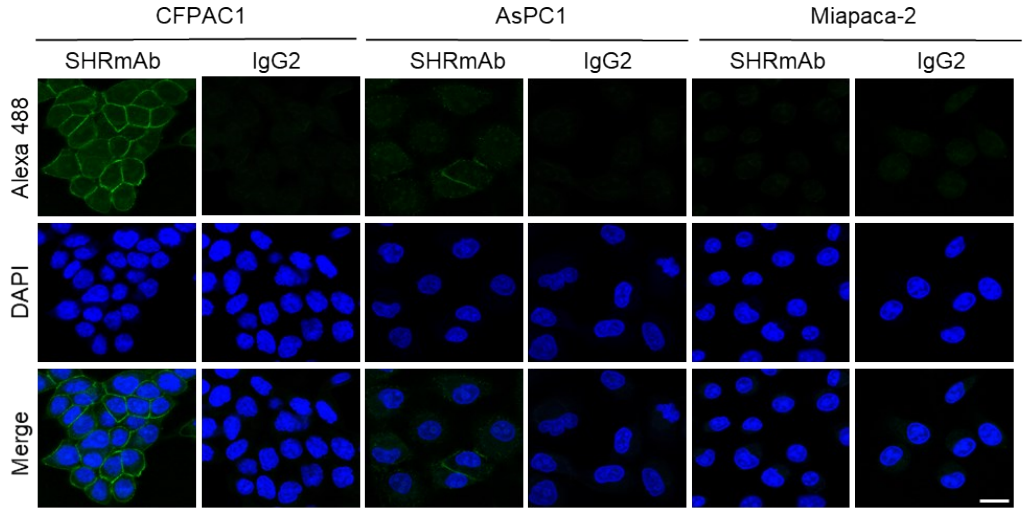

Figure S3. Confocal microscopic images of CFPAC1, AsPC1, and Miapaca-2 after incubation with SHRmAb or IgG2. IgG as isotype control. Scale bar: 20 μm.

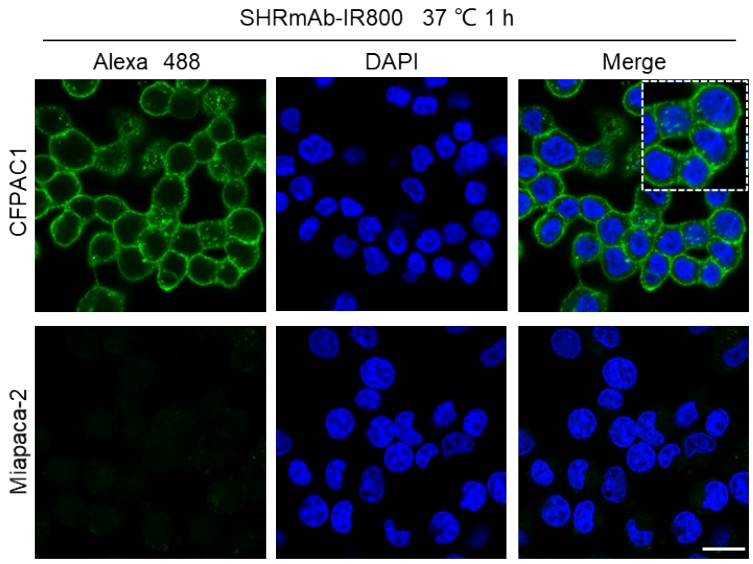

Figure S4. SHRmAb-IR800 was internalized within the cell cytoplasm in CFPAC1 cells, Miapaca-2 cells as negative control. Scale bar: 20 μm.

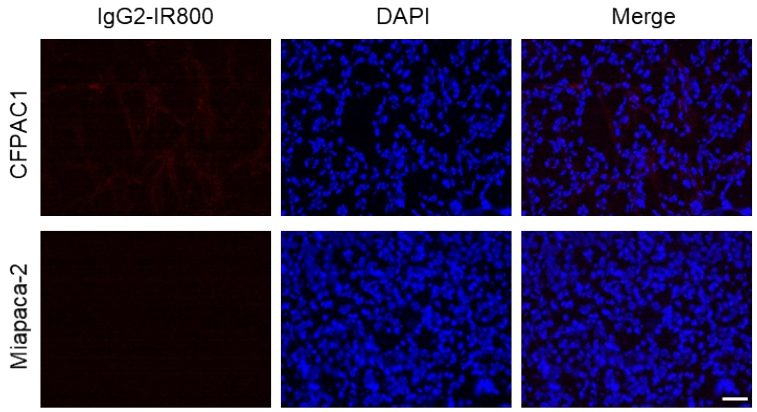

Figure S5. Frozen section analysis of IgG2-IR800 in CFPAC1 and Miapaca-2 tumour tissue. Scale bar: 50 μm.

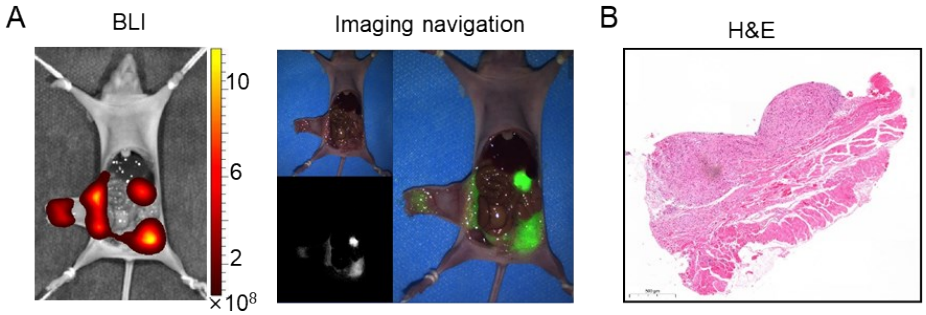

Figure S6. NIRF-guided surgery of the CFPAC1 orthotopic tumour model with seeding metastasis. (A) The BLI (bioluminescence imaging) and NIRF imaging of the model. (B) Post-resection of NIRF-positive tissues under surgical guidance, and H&E staining of pathological biopsy of samples.

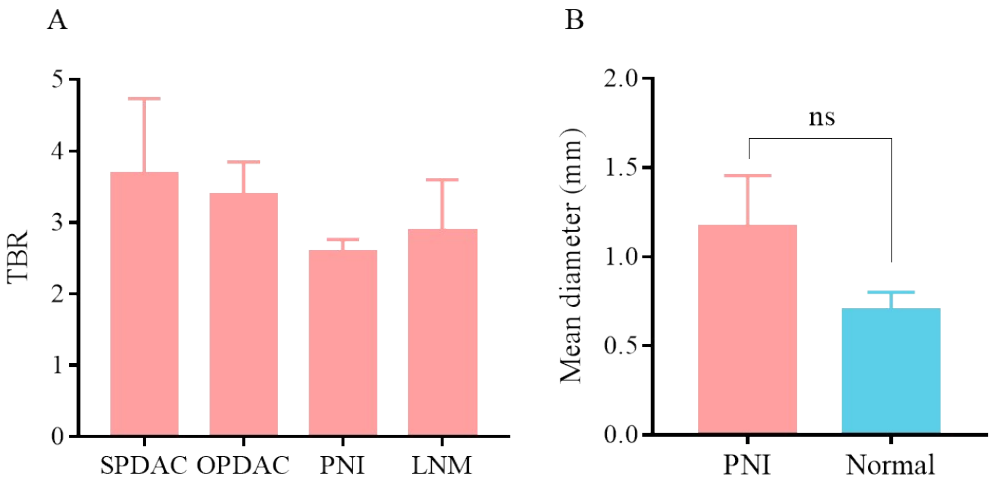

Figure S7. (A) The TBR of subcutaneous PDAC (SPDA), orthotopic PDAC (OPDA), PNI, and LNM. (B) Mean diameter of the PNI lesions and normal nerves. ns: Not significant.